Compressive Sensing Applied to Production Testing of Array Antennas using a Robotic Arm and Very Sparsely Sampled Near-Field Measurements

C.G. Parini[2], S.F. Gregson[1, 2]
[1] Next Phase Measurements LLC, CA, USA, stuart.gregson@qmul.ac.uk
[2] Queen Mary University London, London, UK

***Abstract*— Compressive Sensing (CS) has been deployed in a variety of fields including wideband spectrum sensing, active user detection and antenna arrays. In massive MIMO arrays, CS has been applied to reduce the number of measurements required to verify the arrays excitation in a production environment. All follow the general approach of creating the sparsity needed for CS by subtracting the measured far-field or near-field of the test array from that of a 'gold standard' array measured under identical conditions. In a previous paper [1] the authors have applied CS to planar near-field (PNF) measurements offering a compact test facility well suited to the production environment for these antennas. In that paper the reconstruction of array excitation with a mean square error (MSE) of -30dB was achieved for a 20 x 28 element array antenna at half wavelength spacing using just 1.5% (177 samples) of the samples needed for a conventional NF measurement (12,100 samples) employing classical back projection to the aperture. Critical to the performance is the realization that the CS samples need to be confined to the central region of the NF measurement plane which for a conventional NF to FF planar antenna pattern measurement would offer a massive truncation error. In this paper we address the optimal sampling strategy needed for this NF approach to diagnose arrays with up to a 4% failure rate by employing a statistical performance analysis of the reconstruction accuracy. Previous publications concerning CS based array diagnostics have exclusively studied the reconstructed array element amplitude, in this work we consider both array element amplitude and phase reconstruction performance that is critical in applying the technique to a production environment.**

Index: Compressive sensing, Planar near-field measurements, Array antenna diagnostics.

I. INTRODUCTION

The 5th generation new radio (5GNR) promises circa ten-to-twenty-fold increase in data rate, and this has necessitated the adoption of several important new technologies. Chief amongst these is the move to higher frequency bands, and the adoption of far more complex Massive MIMO (Multiple Input Multiple Output) array antenna architectures and electronic beam scanning, which are needed to handle the associated increase in free-space RF path-loss. Although the frequency band below 6 GHz may be used during the initial rollout, 5G technologies will mainly occupy the 28 GHz, FR2, frequency band, or possibly higher, necessitating the widespread use of more complex, electrically larger, massive MIMO antennas [2, 3]. With the adoption of these more complex phased array antennas (typically comprising many hundreds of elements), comes the need to test and calibrate them as part of the production process. A classical approach would be to measure the field close to each array aperture, or the use of Near-Field/Far-Field (NF/FF) measurements to verify the FF beam or back project into the aperture to verify element excitations [4]. For volume production of massive MIMO arrays such studies need to be undertaken at the development stage leading to the creation of a reference or 'gold' standard antenna which then needs to be replicated in volume. Thus, we need to consider alternative (fast) methods to drastically reduce the number of measurements and the time needed to determine an array's excitation by making use of the known excitations of the 'gold' antenna.

Compressive Sensing (CS) has been deployed in a range of disciplines and works on the principle that we can reconstruct a big space (P), from just a few samples (M) providing we can find an appropriate transform that enables the big space to be defined by only a few variables within this necessarily sparse domain. For the case of antennas, an array of sources can be used to define the fields on a PNF surface using the plane wave spectrum or the equivalent sources method. When using the equivalent sources method [7], the inverse transform from the NF to aperture is the 'compressed sensing' protocol with the key to compressive sensing being recovering the full measurement from the compressed ones by utilizing the sparsity property [5] from a few NF measurements. A review of CS techniques for antenna applications can be found in [6].

In an earlier paper by the authors [1] the basic concept of this CS based PNF array diagnostics using the equivalent currents method is described in detail. To summarise we exploit the fact that the 'gold' reference antenna exists and explore the use of CS to undertake a back transform to the array aperture from the PNF measurement of the difference between the NF pattern of the AUT, and the 'gold' antenna using minimal, randomly located, radiated NF samples. Here, the aim is to minimise the number of measurement points, M, required to reliably and accurately measure the antenna in the NF, whilst accurately reconstructing the array element excitations. This approach is summarised in Fig. 1, where the back projected array excitations indicate just the difference between the excitations of the "defective" production antenna, and the 'gold' reference antenna.

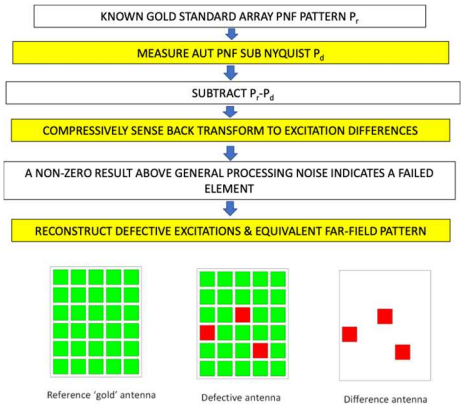

Figure 1. Top: Flow diagram of defective element detection using compressive sensing. Bottom: the 'sparse' difference antenna concept.

II. The Concept of Compressive Sensing

In this section we provide an introduction to sparce sampling and compressive sensing. CS is a way of sampling signals with the prior knowledge that the signals are sparse in some domain. This can be expressed as a linear algebra statement:

- We have fewer equations than unknowns, so there are an infinite number of solutions.
- We can find a solution to an underdetermined linear system of equations on the condition that the solution is sparse, i.e. most elements are zero.
- The method requires incoherent measurements, *i.e.* randomness.

The number of measurements required is dependent on the sparsity of the solution. Only in the last 15 years that advances in applied mathematics and statistics have allowed us to solve this efficiently and robustly for the sparsest [*s*]. The process can be summarized in Fig. 2.

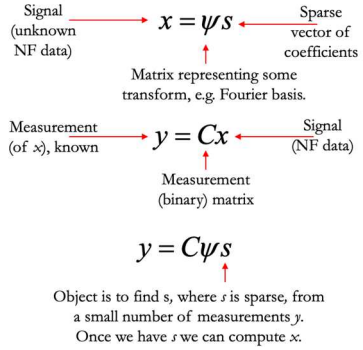

Figure 2. Illustration of the concept of Compressive Sensing.

To illustrate the CS problem we consider Fig. 3, the object is to find *s*, where *s* is sparse, from a small number of measurements *y*. Once we have *s* we can compute *x*. We find *s* by optimizing:

$$\min \|s\|_1 \text{ such that } \|y - C\psi s\|_2 < \sigma \qquad (1)$$

Where *C* needs to be incoherent with respect to ψ, *i.e.* as far away from $C = \psi^{-1}$ as is possible. The term σ^2 is determined by the noise level affecting the measured samples.

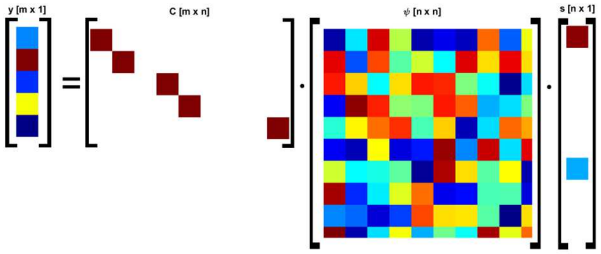

Figure 3. An illustration of CS problem in matrix form, colours denote non-zero complex values and white denotes zeros.

In our case the *y* in Fig. 3 represents sample NF measurements, *C* is the measurement matrix which defines the NF sample point locations, and ψ represents the transform from element current to NF point.

In (1) we use the l_1 norm to minimise *s*, in mathematics, a norm is in some sense a measure of distance [5]. The norm of a vector is its length:

- The l_0 norm is the number of non-zero elements in the vector, this is a measure of the sparsity.
- The l_1 norm is the sum of the absolute value of the entries in the vector (Manhattan distance).
- The l_2 norm is the square root of the sum of the square of the entries in the vector (Euclidean distance).

Here, the value is that the l_1 norm provides the greatest number of zero valued entries, that is to say it produces the sparsest vector [*s*], which is what we are looking for.

A full description of the implementation based on the current elements method, and the cvx based compressive sensing formulation can be found in [1].

III. Measurement Simulations

We first consider a conventional PNF scan of a 20 x 28 element dipole array with half wavelength spacing and operating at 8.2GHz. The scan plane is 2m by 2m with the NF probe distance of 3 λ from the aperture and a measurement noise level set at -60dB from the peak signal level, with NF measurement points separated by half wavelengths (λ/2) in *x* and *y* which results in 12,100 sample points in all. We now add four randomly located faults to this ideal array of the form -6dB and 45°; -10dB and -75°; -30dB and 135°; -3dB and 110° and simulate the defective NF.

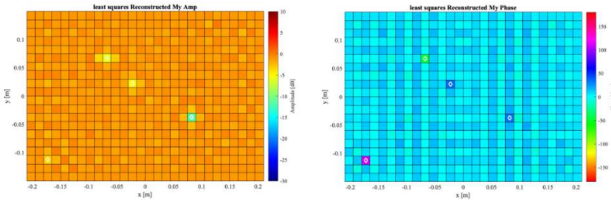

Figure 4. Back transformed array excitations for defective array. Defective elements indicated by white diamond. Left: amplitude, Right: phase.

We can then compute a conventional back transform [7] to the array aperture and obtain the amplitude and phase excitation of the defective array as shown in Fig. 4.

Considering the element excitation as a complex number, the RMS element excitation error over the whole array was 15.5 dB with maximum error of -8.4 dB, this taking account of both amplitude and phase errors as a single performance parameter. The false alarm level (RMS error amplitude calculated over the elements that were not faulty) was -25.7 dB with a maximum of -11.9 dB. From these performance parameters we see that the phase errors are quite well defined, but the amplitude errors are less so, all with a considerable 'background noise' to the excitations meaning small amplitude and phase variations across the AUT array are undetectable.

We now turn our attention to using the CS diagnostic process described above which in this case takes the difference between the near-fields of the reference and defective antennas to create the required sparsity. The resulting reconstructed excitations of the defective array are shown in Figure 5. In this case the RMS element complex excitation error over the whole array was -31.7 dB with maximum error of -9.4 dB and the RMS false alarm level was -39.9 dB with a maximum of -19.2 dB. This performance is considerably better than that which would be obtained using conventional back projection results with very evident lower background noise (low false alarm level). Crucially this was achieved with just 177 NF samples, which is just 1.5% of the conventional back projection case of 12,100 samples Nyquist spaced ($\lambda/2$) apart. This level of performance has been achieved by making many modifications to the very basic application of CS, which would simply be: randomly choosing a number of sample points, M, from the 12,100 conventional NF sample plane and applying the CS algorithm just once. In the remainder of this section, we will describe these modifications and the level of performance achievable.

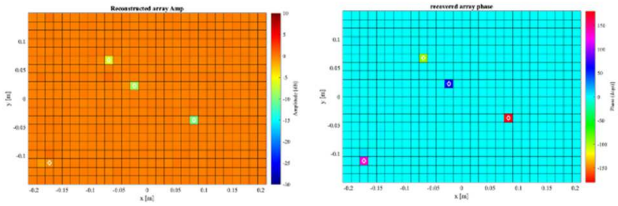

Figure 5. CS based reconstruction of array amplitude excitations for defective array. Defective elements indicated by white diamond. Left: amplitude, right: phase.

Modification 1: choice of NF region:- The most crucial modification is the realization that the CS samples need to be confined to the *central* high intensity field region of the NF measurement plane, which is effectively the projection of the array aperture, as shown by the white rectangle in the NF phase plot of Fig. 6. For a conventional NF back projection process such a data truncation would offer massive truncation error. In both cases, these measurement simulations were taken with each NF point being subject to -60dB of background noise.

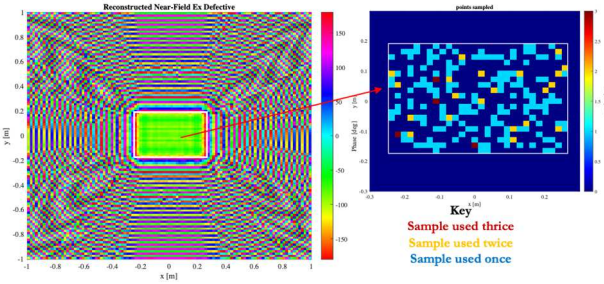

Figure 6. Left: NF phase of defective array showing sample space as white rectangle. Right: NF samples taken in optimal central NF region only, 36 random points repeated six times.

Modification 2: smart sampling:- Taking M purely randomly located samples within the sample region of Fig. 6 results in clusters of points and relatively large empty spaces between samples leading to a mediocre reconstruction performance. However, a completely periodic sampling of the sample region would lead to gross aliasing and should always be avoided when using CS techniques. Here we employ a Poisson like sampling approach for the M samples. In Fig. 6 each set of M=36 samples are pseudo-randomly selected within the sample space, and this is achieved by dividing the sample space into 36 equal size rectangles and then randomly selecting one sample point within each rectangle.

Modification 3: Run CS process several times with different sample sets:- For the case shown in Fig. 6 we take multiple sets of 36 samples, run the CS algorithm each time and then take the complex average of the recovered array element excitations. As demonstrated in [1] we have found that taking six sets of 36 samples offers a good compromise between performance and number of samples required. This process means that some samples points are used more than once (see Fig. 6) and this results in the total number of unique samples being taken as 183 in the case of Figure 6 rather than $36 \times 6 = 216$. In a real-life measurement, these six sets of 36 samples can be determined a priori and so the desired unique measurement points can then be measured using a robotic arm mounted NF probe.

With these modifications in place, we need to determine the level of reconstruction performance, so we take a far broader statistical view by running a random selection of fault locations many times, and plot the cumulative distribution function (CDF) [1] of the mean square error (MSE). Fig. 7 shows the CDF MSE over 50 runs in the presence of -60 dB noise for the array of Fig. 5. If we take the 80% CDF MSE level as a useful reference point to compare results (*i.e.* 80% of the runs will be better than or equal to this MSE value), then this result shows a MSE of -33.1 dB. We have taken the 80% CDF point rather than the one-sigma (68%) point, or the two-sigma (95%) as arguably it provides a fairer representation of system performance. Also shown on this figure is the CDF MSE of just the faulty

elements, which for this case is -12.8 dB at the 80% point. The CDF of the maximum value of the excitation error for each run is also shown in Figure 7 and at the 80% CDF point is -10 dB.

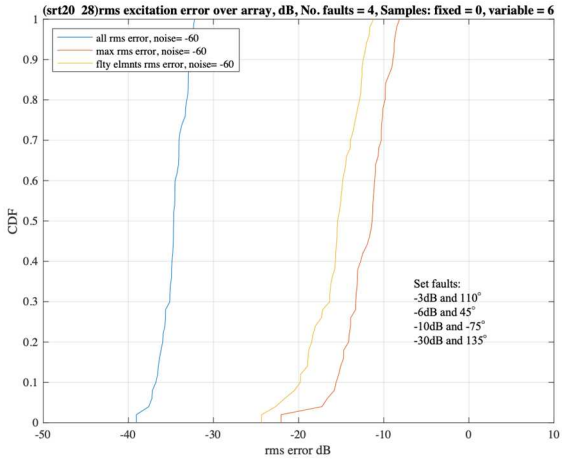

Figure 7. CDF of amplitude excitation error with statistics taken over 50 random sets of 4 fault locations. Faults fixed as shown in the inset table.

We should point out that, unlike some publications, the faults we simulate are faults of *both* amplitude and phase (see inset to Fig. 7), and we are measuring the quality of the reconstruction of both array element amplitude *and* phase excitation. Our aim is not to just detect whether an element is on or off, but rather to reconstruct the array excitations as accurately as possible with the smallest number of samples. Clearly, reconstruction performance deteriorates as the number of faults increases, but this can be partly compensated by increasing the number of samples, *M*.

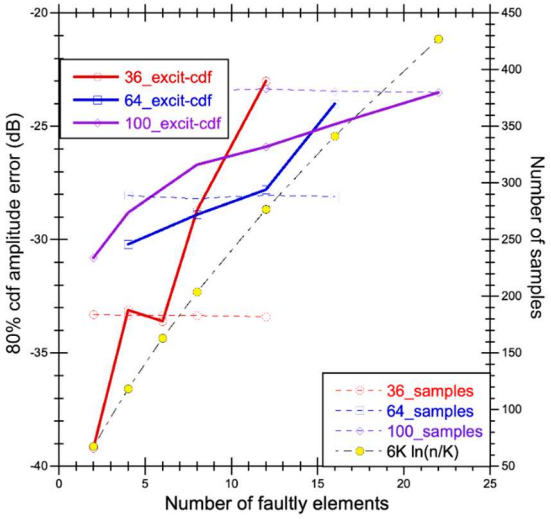

Figure 8. 80% CDF MSE of reconstructed array amplitude vs the number of faulty elements for different number of samples per set, with six sets used to determine the reconstruction. The average number of samples needed for each M case is shown on the right hand scale.

To aid in the choice of *M* we have repeated the process that produced the results of Fig. 7 using different numbers of faulty elements *K*, and samples *M* and have plotted the 80% CDF MSE value of the array excitation amplitude in Fig. 8.

In all cases each of the 50 statistical runs took six sets of *M* samples as previously described. The number of samples on the right-hand side of Fig 8 is then the average number of samples needed for each of the 50 runs.

From Fig. 8 it is evident that prior knowledge of the number of faults to expect from the AUT is crucial in determining the number of samples needed. If the array has an expected failure rate of 1% (6 faults in this case) then we need to take around 183 samples (1.5% of Nyquist needed for classical back projection). However, if we are expecting a failure rate of 4% (22 faults) then we need to take a larger number of around 380 samples (3.1% of Nyquist). To illustrate a possible practical scenario, we take our 20x28 array and apply a full failure of one complete column (20 faults) and in addition add two other elements with just a 90° phase faults giving a total of 22 faults. We run the CS procedure with *M*=100 per run, with six runs requiring typically 380 samples (from Fig. 8), which is 3.1% of Nyquist. Fig. 9 shows both the true faulty array and the resulting reconstruction. Both the faulty column and the two outlying phase faults are clearly evident in the reconstruction. The accuracy of the amplitude reconstruction of the faulty column is poor, but clearly indicates that the array has a faulty column. The accuracy to which the two outlying 90° phase errors are recovered is excellent however, with reconstructions of 105° and 107°. Also evident for these two phase errors is the bleed-thro seen on the reconstructed amplitude (+1.6 and +2.7) dB of those two elements as well as some fractional amplitude errors surrounding these fault locations. With these faults corrected we then check this array with a second CS scan this time using *M*=36 (189 samples) as we expect few faults. The resulting reconstructed array is indistinguishable from the reference array with an amplitude MSE level -62dB with a maximum error of -46dB and phase MSE level of 0.04° with a maximum of 0.3°.

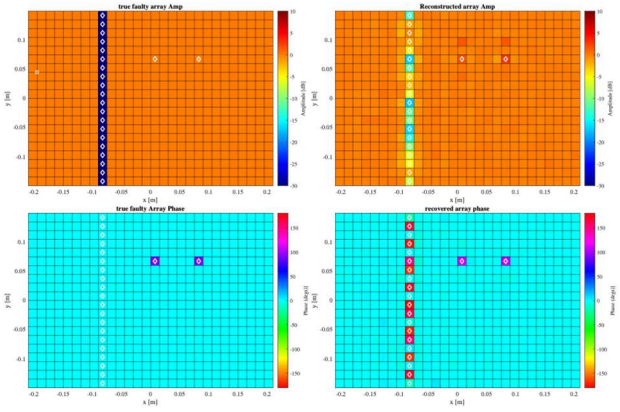

Figure 9. Left column: true array excitation with a full column fault (elements set to -40dB) plus two faults of phase at +90°; Right column: reconstructed array excitation. Top amplitude, bottom phase.

Fig. 8 also shows an estimation of the number of samples needed for a given array size n and number of faults K using the formula K_1*ln(n/K) where K_1 is a constant of around 5-6. This formula is often used in the wider compressive sensing field [5] and is clearly a good estimation for this work.

We have found that to get the best performance from this CS array diagnostics the reference and AUT arrays are best tested with a uniform amplitude excitation to maintain the best signal to noise (S/N) of the resulting difference complex field pattern that represents the sparse array that CS is applied to. An array with a tapered amplitude distribution just creates a poorer S/N at the edges of the array. As we are taking the difference NF pattern between reference and AUT the phase used is immaterial, in the above results we have used a flat phase, but we have tested both a scanned beam phase distribution and a random phase distribution and equally good results are obtained.

Finally, it is important to realise what these low percentage level of element faults cause to the far-field (FF) pattern. In Fig.10 we plot the azimuthal FF patterns for the 20x28 array for the case with 8 faults and 22 faults (1.4% and 4% failure rate respectively) along with the equivalent multipath level (EMPL). Looking at these FF patterns it would be difficult to determine that the array has any fault at all using purely FF measurements. It is also worth noting that the directivity loss for 8 faults is just 0.12dB, and for 22 faults is still only 0.34dB.

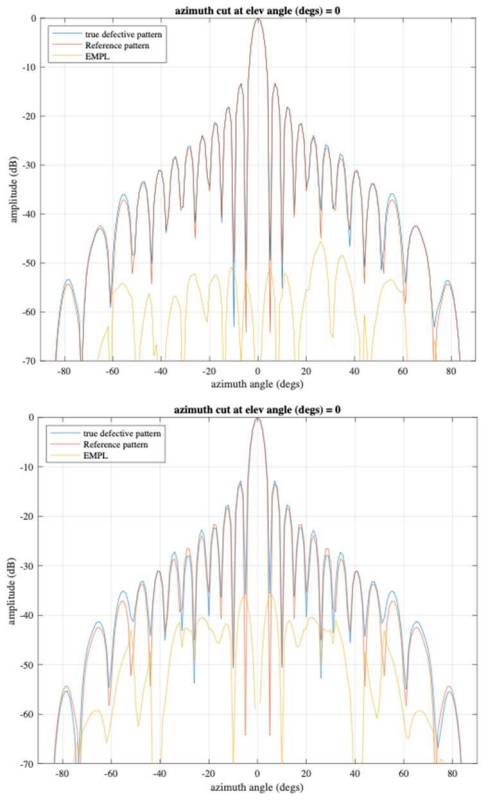

Figure 10. FF azimuth radiation pattern difference between reference and defective array with; top: 8 faulty elements; bottom: 22 faulty elements.

IV. Summary, Conclusions and Future Work

This works builds on our earlier publications [1, 6] in the use of conventional convex optimisation-based CS in array diagnostics. Many of the techniques developed for PNF array diagnostics were developed for use in far-field (FF)-multiprobe anechoic chamber (MPAC) testing [6]. However, PNF is much better suited to a production test environment where the predetermined NF sample locations (based on simulated measurements and expected element failure rate) can be easily**,** rapidly**,** and flexibl***y*** taken using an industrial robotic arm in a compact space.

Our results, summarised in Fig. 8, have shown the level of reconstruction possible for a given set of sparse samples and the number of faulty array elements. We have demonstrated that both amplitude and phase excitation of the array can be well reconstructed. We have covered a wide range of sample to element ratio (M/n) of up to about 0.6. Depending on the level of reconstruction accuracy we have found that arrays with up to 4% element failure rate are suitable for this CS based diagnostics. This level of failure is compatible with what could be expected to be encountered in a typical massive MIMO arrays production facility. In [8] the Bayesian Compressive Sensing (BCS) framework was applied to this 'gold' array comparison approach. The work demonstrated that diagnostic errors of order -30dB are achievable with NF measurement to element ratio (M/n) of >0.6. BCS is however more complicated to use, requiring several control parameters to be predetermined before use. In our future work we aim to be comparing and contrasting these two methods for production testing applications.

References

[1] C.G. Parini, S.F. Gregson, "Compressive Sensing Applied to Planar Near-Field Based Array Antenna Diagnostics for Production Testing", AMTA 2023, October 2023, Seattle, USA.

[2] Wonil Roh, "5G Mobile Communications for 2020 and Beyond - Vision and Key Enabling Technologies," *IEEE WCNC 2014 Keynote*, Apr. 2014.

[3] Z. Pi and F. Khan, "An introduction to millimeter-wave mobile broadband systems," *IEEE Commun. Mag.*, vol. 49, no. 6, pp. 101–107, Jun. 2011.

[4] C. G. Parini, S. F. Gregson, J. McCormick, D. Janse van Rensburg "Theory and Practice of Modern Antenna Range Measurements", *IET Press,* 2014, ISBN 978-1-84919-560-7. (second edition published in 2021)

[5] S.L. Brunton, J.N. Kutz, "Data-Driven Science and Engineering", second edition, Cambridge University Press, 2022, ISBN 978-1-009-09848-9

[6] S.F. Gregson, Z. Qin, C.G. Parini, "Compressive Sensing in Massive MIMO Array Testing: A Practical Guide", IEEE Transactions on Antennas and Propagation, 2022, Volume: 70, Issue: 9

[7] S.F. Gregson, J. McCormick, C.G. Parini, "Principles of Planar Near-Field Antenna Measurements, 2nd Edition", IET Electromagnetic Waves series 53, ISBN 978-1-83953-699-1, July 2023.

[8] Z. Lin, Y. Chen, X. Liu, R. Jiang and B. Shen, "A Bayesian Compressive Sensing-Based Planar Array Diagnosis Approach From Near-Field Measurements," in *IEEE Antennas and Wireless Propagation Letters*, vol. 20, no. 2, pp. 249-253, Feb. 2021, doi: 10.1109/LAWP.2020.3046879.